RAPID COMMUNICATION

μSR and NMR studies on the van der Waals cluster magnet Nb_3Cl_8

To cite this article: Lin Yang *et al* 2025 *Chinese Phys. B* **34** 057501

RAPID COMMUNICATION

μSR and NMR studies on the van der Waals cluster magnet Nb_3Cl_8

Lin Yang(杨林)[1,2,†], Detong Wu(吴德桐)[3,4,1,†], Xin Han(韩鑫)[1,2], Jun Luo(罗军)[1,2], Bo Liu(刘波)[1], Xiaoyan Ma(马肖燕)[1], Huiqian Luo(罗会仟)[1], Jie Yang(杨杰)[1], Bing Shen(沈冰)[3,4], Rhea Stewart[5], Devashibhai Adroja[5], Youguo Shi(石友国)[1,6,7,‡], Rui Zhou(周睿)[1,§], and Shiliang Li(李世亮)[1,2,7,¶]

[1] *Beijing National Laboratory for Condensed Matter Physics, Institute of Physics, Chinese Academy of Sciences, Beijing* 100190, *China*
[2] *School of Physical Sciences, University of Chinese Academy of Sciences, Beijing* 100190, *China*
[3] *Center for Neutron Science and Technology, Guangdong Provincial Key Laboratory of Magnetoelectric Physics and Devices, School of Physics, Sun Yat-Sen University, Guangzhou* 510275, *China*
[4] *State Key Laboratory of Optoelectronic Materials and Technologies, Sun Yat-Sen University, Guangzhou* 510275, *China*
[5] *ISIS Neutron and Muon Source, Rutherford Appleton Laboratory, Chilton, Didcot, OX*11 0*QX, UK*
[6] *Center of Materials Science and Optoelectronics Engineering, University of Chinese Academy of Sciences, Beijing* 100049, *China*
[7] *Songshan Lake Materials Laboratory, Dongguan* 523808, *China*

(Received 12 March 2025; revised manuscript received 27 March 2025; accepted manuscript online 28 March 2025)

The van der Waals cluster magnet Nb_3Cl_8 has recently been shown to possibly host a quantum-spin-liquid ground state. The Nb ions in this compound form a breathing kagome structure, where the magnetic moment comes from three nearest Nb ions forming a molecular cluster with spin 1/2. Previous bulk measurements including magnetic susceptibility and specific heat suggested the existence of spinon Fermi surfaces. Here we further probe the spin system by nuclear magnetic resonance (NMR) and muon spin rotation and relaxation (μSR) techniques. We confirm that there is no magnetic long-range order and the dynamical spin fluctuations persist down to 0.075 K. These results provide further evidence that Nb_3Cl_8 may host a quantum spin liquid.

Keywords: quantum spin liquids, cluster magnet, spin excitations

PACS: 75.10.Kt, 76.75.+i, 74.25.nj

DOI: 10.1088/1674-1056/adc667 **CSTR:** 32038.14.CPB.adc667

Quantum spin liquids (QSLs) represent a class of phases where quantum spins are highly correlated yet do not order at very low or zero temperature.[1–4] While the exact definition of QSLs is still lacking, the kagome structure has been treated as one of the most important platforms to search for QSLs due to its strong geometrical frustrations.[5] Apart from the perfect one, the breathing kagome structure has also attracted increasing interest theoretically.[6–13] In this structure, the bond length changes alternately within the hexagon, resulting in two kinds of triangles with different bonds, as shown in Fig. 1(a). Different from the perfect kagome lattice, where each site hosts a magnetic moment, three magnetic ions on the breathing kagome lattice can form a cluster with delocalized unpaired electrons to give a net magnetic moment. These structures have been found in $(NH_4)_2[C_7H_{14}N][V_7O_6F_{18}]$(DQVOF),[14,15] Mo_3O_{13}-cluster-based materials (e.g., $LiZn_2Mo_3O_8$, $Li_2ScMo_3O_8$, $Li_2In_{1-x}Sc_xMo_3O_8$, and $Na_3Sc_2Mo_5O_{16}$),[16–22] and Nb_3X_8 (X = Cl, Br, I).[23–28] Many of them show no magnetic order down to the lowest measurable temperatures and thus are promising QSL candidates.

In Nb_3Cl_8 with a trigonal structure at room temperature, Nb ions form breathing kagome layers that are connected by weak van der Waals force.[23,24] At high temperatures, it is a Mott insulator that can be well described by the single-band Hubbard model.[25–27] The system exhibits paramagnetism at high temperatures with an effective moment of approximately $1.7\mu_B$ per three Nb ions, which corresponds to $S = 1/2$.[23,24] This is explained by the Nb_3 trimers, i.e., the small triangles formed by the three nearest Nb ions, as shown in Fig. 1(b). Since the intra-trimer and inter-trimer Nb–Nb bond distances are about 2.81 Å and 3.93 Å, respectively, the bonding within the trimer is believed to be metallic. Therefore, the trimer should be treated as a whole with a valence state of $[Nb_3]^{8+}$, comprising seven d electrons, which results in $S = 1/2$. Since the trimers form a triangular lattice, it might be argued that the magnetism should be understood as a 2D triangular lattice too. While the system becomes non-magnetic below a structural transition around 100 K, the magnetism can be retained in powders or polycrystals, and heavily c-axis pressed

[†]These authors contributed equally to this work.
[‡]Corresponding author. E-mail: ygshi@iphy.ac.cn
[§]Corresponding author. E-mail: rzhou@iphy.ac.cn
[¶]Corresponding author. E-mail: slli@iphy.ac.cn

single crystals that destroy the structural transition.[29] Intriguingly, magnetic susceptibility and specific-heat measurements suggested the existence of a possible QSL with spinon Fermi surfaces.[29] This seems at odds with the Heisenberg model on the triangular lattice, whose ground states are magnetically ordered,[3] considering that there should be no large anisotropy and no long-range interactions in this system. On the other hand, models on the breathing kagome lattice with 1/6 electron filling have predicted various kinds of QSLs, including those with spinon Fermi surfaces.[6,7,11,12]

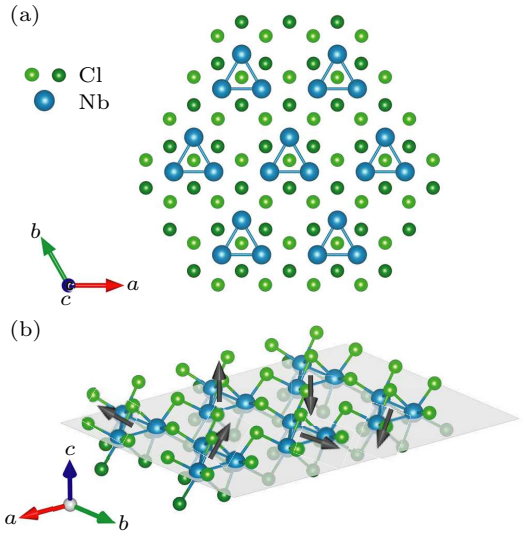

Fig. 1. (a) Top view of the monolayer of Nb_3Cl_8 showing the breathing kagome structure of Nb_3 trimers. Light and dark green spheres represent the Cl atoms above and below the Nb layer, respectively. (b) Schematic picture of monolayer Nb_3Cl_8 with a frustrated $S = 1/2$ magnetic moment centered in the $[Nb_3]^{8+}$ trimer.

In this work, we further study the magnetic ground state of polycrystalline Nb_3Cl_8 with the trigonal structure by both NMR and μSR techniques. The $1/T_1T$ of the NMR spectra shows a Curie–Weiss temperature dependence with a nearly zero Weiss temperature. The μSR measurements show that there is no magnetic ordering down to 0.075 K. Moreover, the relaxation rate shows no change below about 1 K and the dynamic part persists at longitudinal magnetic fields, suggesting the QSL ground state of Nb_3Cl_8.

To avoid the structural transition that leads to a nonmagnetic state at low temperatures, we utilized a polycrystalline Nb_3Cl_8 sample for our study.[29] Polycrystalline Nb_3Cl_8 was synthesized by solid-state reactions. High-purity Nb powder (Alfa Aesar, 99.99%) and $NbCl_5$ powder (Alfa Aesar, 99.9%) were thoroughly mixed using a mortar and pestle in a molar ratio of 7:8 and placed in an alumina crucible. The crucible was then sealed in a quartz tube under vacuum, heated at 700 °C for 48 hours, and naturally cooled to room temperature. NMR measurements were conducted using a phase-coherent pulsed NMR spectrometer. The spectra were obtained by integrating the spin echo as a function of frequency at $B_0 = 7.53$ T. The spin-lattice relaxation rate T_1 was measured by using the saturation–recovery method and determined by fitting to the theoretical curve. The μSR measurements were carried out using the MuSR spectrometer with a dilution refrigerator (DR) (0.075–2.0 K) and Variox cryostat (1.8–4.0 K) at the ISIS Facility, Rutherford Appleton Laboratory, UK. The polycrystalline Nb_3Cl_8 samples were placed in a standard 30×30 mm thin silver sample holder. Measurements were performed in the longitudinal geometry of the μSR spectrometer in true zero magnetic field (ZF) and in applied longitudinal fields (LF) with respect to the initial muon spin polarization. A 20 Oe weak transverse field (wTF) calibration measurement was also performed.

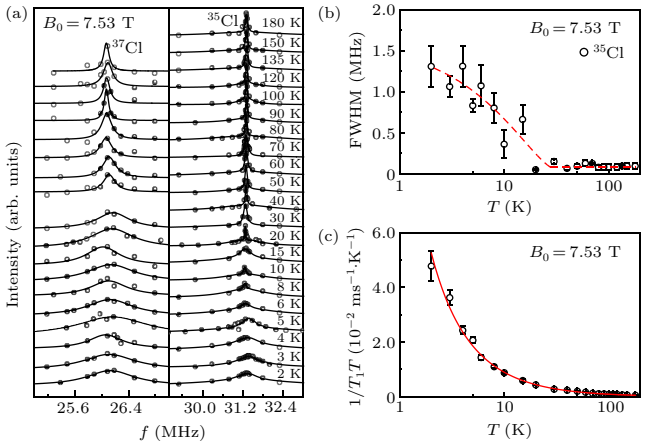

Fig. 2. (a) The left and right panels display ^{37}Cl- and ^{35}Cl-NMR spectra at an external field $B_0 = 7.53$ T for various temperatures, respectively. Solid lines represent the fit by Lorentzian function. (b) The temperature dependence of FWHM of ^{35}Cl-NMR line. The dashed line is a guide to the eye. (c) The temperature dependence of $1/T_1T$ measured at the ^{35}Cl-NMR line. The solid line is the fit result using Eq. (1) as described in the text.

We start with the NMR results on the chlorine. Since both ^{35}Cl and ^{37}Cl nuclei, with spin $I = 3/2$, have a nuclear quadrupole moment that couples to the electric field gradient, three sets of NMR lines would be detected in their NMR spectra. However, for the polycrystalline sample, the orientation of grains is random without any preferred direction. The distribution of the angle between the applied magnetic field and the c-axis results in spectrum broadening. As a result, only one broad peak is observed in both ^{35}Cl and ^{37}Cl NMR spectra, as shown in Fig. 2(a). No change in the spectra is observed around 100 K, demonstrating that the structural transition is indeed suppressed.[29] Below about 30 K, both spectra become broader. Figure 2(b) shows the temperature dependence of the full width at half maximum (FWHM) of the ^{35}Cl NMR line, suggesting the enhancement of magnetic fluctuations at low temperatures. Note that the existence of spin glass below 20 K has been ruled out by the magnetic-susceptibility measurements reported previously.[23,24,29] The broadening of the NMR spectra at low temperatures most likely originates from the short-range order due to quenched disorders as observed in other QSL candidates.[30] Figure 2(c) shows the temperature dependence of $1/T_1T$, which can be well fitted by the

Curie–Weiss function

$$\frac{1}{T_1T} = \left(\frac{1}{T_1T}\right)_0 + \frac{C}{T-\theta}, \tag{1}$$

where $(1/(T_1T))_0$ is the contribution from the density of states at Fermi level, which is extremely small for this insulating sample. The value of θ is -0.37 ± 0.23 K, very close to zero, suggesting that the staggered susceptibility tends to diverge at zero temperature, at least down to 2 K.

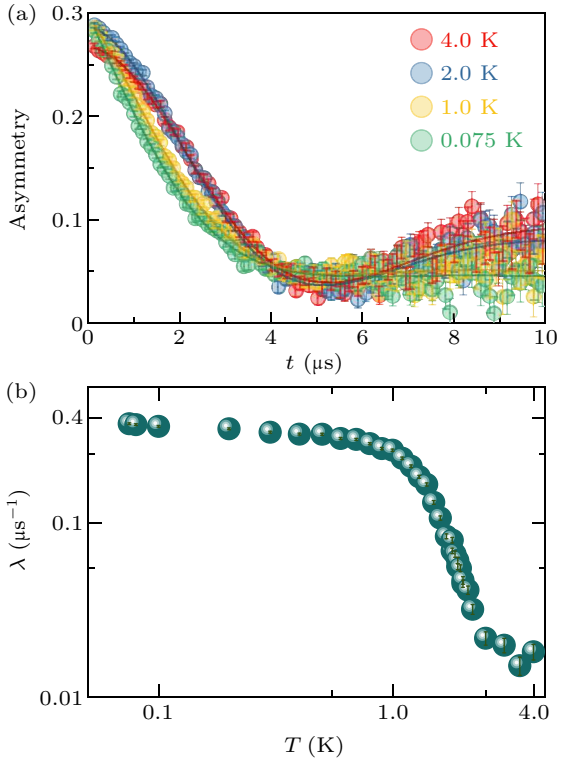

Fig. 3. (a) Time dependence of characteristic μSR spectra at zero field at 0.075 K, 1.0 K, 2.0 K and 4.0 K, respectively. Solid lines are fitted results by Eq. (4). (b) Temperature dependence of the relaxation rate λ.

To further study the spin system of Nb_3Cl_8, we measured the μSR spectra under both ZF and LF conditions at various temperatures. Figure 3(a) shows some of the ZF results, where neither oscillations nor a significant drop in initial asymmetry is observed, indicating the absence of long-range magnetic ordering. We use a static Kubo–Toyabe polarization function $G_{\rm KT}(B_{\rm L},\Delta,t)$ multiplied by a stretched exponential relaxation function to fit both ZF and LF data:[31,32]

$$A_{\rm ZF/LF}(t) = AG_{\rm KT}(B_{\rm L},\Delta,t)\,{\rm e}^{-(\lambda t)^{\beta}} + A_{\rm bg}, \tag{2}$$

where A is the initial asymmetry, Δ/γ_μ is the standard deviation of the static field distribution, γ_μ is the muon gyromagnetic ratio $2\pi \times 135.5$ MHz$\cdot$T^{-1}, λ represents the relaxation rate, and $A_{\rm bg}$ is a constant background. For LF measurements with field $B_{\rm L}$, the static-Gaussian-longitudinal-field Kubo–Toyabe function is

$$G_{\rm KT}(B_{\rm L},\Delta,t) = 1 - \frac{2\Delta^2}{\gamma_\mu^2 B_{\rm L}^2}\left(1-{\rm e}^{-\frac{1}{2}\Delta^2t^2}\cos(\gamma_\mu B_{\rm L}t)\right) + \frac{2\Delta^4}{\gamma_\mu^3 B_{\rm L}^3}\int_0^t {\rm e}^{-\frac{1}{2}\Delta^2\tau^2}\sin(\gamma_\mu B_{\rm L}\tau){\rm d}\tau. \tag{3}$$

At zero field, equation (3) reduces to the static-Gaussian-zero-field Kubo–Toyabe function as

$$G_{\rm KT}(0,\Delta,t) = \frac{1}{3} + \frac{2}{3}\left(1-\Delta^2t^2\right){\rm e}^{-\frac{\Delta^2t^2}{2}}. \tag{4}$$

The ZF asymmetry $A_{\rm ZF}(t)$ at all measured temperatures are in good agreement with Eq. (2) with $\beta = 1$. Note that the values of the initial asymmetry A are different in the DR and the Variox cryostat, without any loss of the initial asymmetry. The analyses show that both A and $A_{\rm bg}$ are very weakly temperature and field dependent ($A \approx 0.25$ and $A_{\rm bg} \approx 0.04$ in the DR, and $A \approx 0.23$ and $A_{\rm bg} \approx 0.03$ in the Variox cryostat). The value of Δ/γ_μ is 3.80 (0.03) Oe and essentially temperature independent, showing that it is related to the nuclear static field.[32] The temperature dependence of λ is shown in Fig. 3(b). From 4 K down to 1 K, a slowing down of spin fluctuations is observed, indicating an enhancement of short-range interactions as T decreases.

The LF-μSR asymmetry spectra under selected external applied longitudinal fields $B_{\rm L}$ at 4.0 K, 1.8 K and 0.075 K are displayed in Figs. 4(a), 4(b), and 4(c), respectively. The LF asymmetry $A_{\rm LF}(t)$ under 0 Oe $< B_{\rm L} <$ 40 Oe can be well fitted by Eqs. (2) and (3). The initial asymmetry A, Δ and the constant background $A_{\rm bg}$ are set the same as those in the ZF analysis. A field of 40 Oe (10 times Δ/γ_μ) could decouple the static fields at all temperatures, but the dynamic part still exists up to 2000 Oe at 0.075 K, suggesting the important role played by the dynamic spin fluctuations. When $B_{\rm L} \geq 40$ Oe, the spectra $A_{\rm LF}(t)$ can be described by the stretched exponential relaxation function since $G_{\rm KT}(B_{\rm L},\Delta,t) \approx 1$,

$$A_{\rm LF}(t) = A{\rm e}^{-(\lambda_{\rm LF}t)^{\beta}} + A_{\rm bg}. \tag{5}$$

Here, $\lambda_{\rm LF}$ is the relaxation rate, β is the stretching exponent. The initial asymmetry A and the constant background $A_{\rm bg}$ remain unchanged. The stretching exponent β can be fixed as 1 at 4.0 K, and fitted to be 0.89 (0.16) and 0.74 (0.14) at 1.8 K and 0.075 K, respectively. The field dependence of $\lambda_{\rm LF}$ at 4.0 K, 1.8 K and 0.075 K is shown in Fig. 4(d).

For a fast-fluctuating spin dynamic system with the field fluctuation rate ν, time correlation of spins $S(t)$ takes the form $S(t) \sim \exp(-\nu t)$ and $\lambda_{\rm LF}(B_{\rm L})$ can be described by the Redfield formula $\lambda_{\rm LF}(B_{\rm L}) = 2\Delta^2\nu/(\nu^2+\gamma_\mu^2B_{\rm L}^2)$, where $\Delta^2 = \gamma_\mu^2\langle\delta B^2\rangle$.[33] However, in our case, $\lambda_{\rm LF}(B_{\rm L})$ cannot be fitted well by the Redfield model, suggesting a more general spin autocorrelation function $S(t) \sim (\tau/t)^x\exp(-\nu t)$.[34–37] Here, τ and $1/\nu$ are the early-time and late-time cutoffs, and x is the power of the correlation function. $\lambda_{\rm LF}(B_{\rm L})$ can be derived by the general expression, as shown in Fig. 4(d),

$$\lambda_{\rm LF}(B_{\rm L}) = 2\Delta^2\int_0^{\infty}\left(\frac{\tau}{t}\right)^x{\rm e}^{-\nu t}\cos(\gamma_\mu B_{\rm L}t){\rm d}t, \tag{6}$$

where Δ/γ_μ is the standard deviation of the local fields distribution, and τ is an early time cutoff introduced to normalize the correlation at $t = 0$. The solid lines in Fig. 4(d) denote the fits using Eq. (6) with $x = 0.40$, 0.59, 0.36, and $\nu = 0.5$ MHz, 1.2 MHz, 3.0 MHz at 4.0 K, 1.8 K, 0.075 K, respectively. This shows the spin autocorrelation function $S(t)$ decays like a power law at low temperatures, which attenuates much slower than the exponential function,[34–36,38] indicating the development of long-time spin correlations.

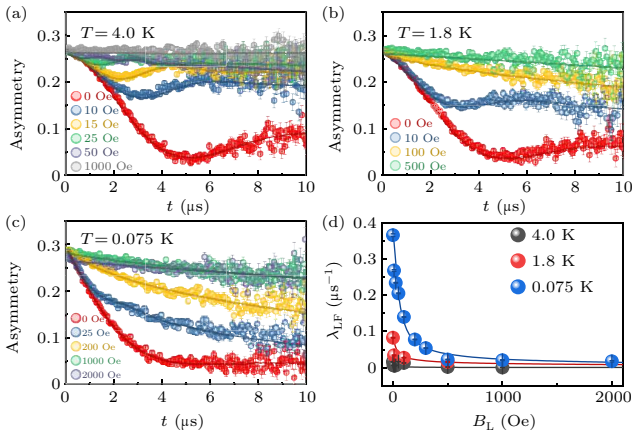

Fig. 4. Time dependence of longitudinal field μSR asymmetry spectra at (a) 4.0 K, (b) 1.8 K, and (c) 0.075 K in selected external magnetic fields. The solid lines are fitted results by Eqs. (3) and (5). (d) Field dependence of the muon spin relaxation rate $\lambda_{\rm LF}(B_{\rm L})$. The solid lines denote the fits using Eq. (6) with $x = 0.40$, 0.59, 0.36, and $\nu = 0.5$ MHz, 1.2 MHz, 3.0 MHz at 4.0 K, 1.8 K, 0.075 K, respectively.

These results, combined with our previous thermodynamic measurements, demonstrate that Nb_3Cl_8 exhibits magnetic properties consistent with the expectation of a QSL, or more precisely, a QSL with spinon Fermi surfaces, when its high-temperature structure is preserved. Firstly, the nearly zero value of θ in the Curie–Weiss fit of $1/T_1T$ from NMR spectra suggests no magnetic ordering down to very low temperatures, which is confirmed by the μSR measurements down to 0.075 K and aligns with the previously reported low-temperature specific heat results.[29] Secondly, other potential disordered states, such as spin-glass or random singlet phases, have been ruled out by prior magnetic-susceptibility and specific heat measurements. Additionally, the LF μSR results in this work also eliminate trivial quantum paramagnetism without strong spin correlations, since the failure of fitting by the Redfield formula for the LF μSR spectra and the introduction of Eq. (6) clearly demonstrate that the spin system is highly correlated spatiotemporally at very low temperatures, consistent with the possible QSL state, as suggested by Ref. [37]. Moreover, the temperature independence of λ has also been widely found in many QSL candidates.[36,37,39–47] Thirdly, the QSL state in Nb_3Cl_8 probably hosts spinon Fermi surfaces, as previous results have shown temperature-independent magnetic susceptibility and linear temperature dependence of specific heat, and a Wilson ratio $R_{\rm w}$ close to 1.[29] Notably, the sharp increase of λ below about 2 K [Fig. 3(b)] seems to happen simultaneously with the low-temperature hump in C/T,[29] indicating that spin fluctuations play a dominant role in different techniques. Whether these behaviors can be unified under the picture of spinon Fermi surfaces needs to be further studied.

While the above discussions have followed traditional approaches to demonstrating a QSL state, it should be noted that any method, including μSR and NMR, cannot provide crucial information for the QSL alone. Results from different experimental techniques and theoretical calculations have to be compared and combined to obtain a unified picture. Our current work suggests the importance of further study using more experimental methods, such as Raman and inelastic neutron scattering. The possible QSL state may also support models on the breathing kagome lattice with 1/6 electron filling,[6,7,11,12] instead of those based on cluster magnets (a triangular lattice for Nb_3Cl_8). Notably, compared to many other QSL candidates, Nb_3Cl_8 may have two advantages. First, its band structure can be readily described by the single-band Hubbard model, which could lead to a better theoretical understanding compared to other more complicated systems. Second, the fact that Nb_3Cl_8 is a van der Waals material could make it easier to apply methods that have been used in two-dimensional systems to provide more solid evidence for the QSL or even an opportunity to develop devices.

Acknowledgments

Project supported by the National Key Research and Development Program of China (Grant Nos. 2022YFA1403800, 2022YFA1403400, 2021YFA1400400, 2023YFA1406100, and 2024YFA1409200), the National Natural Science Foundation of China (Grant Nos. 12274444, 12374142, and 12304170), and the Chinese Academy of Sciences President's International Fellowship Initiative (Grant No. 2025PG0007). A portion of this work was carried out at the Synergetic Extreme Condition User Facility (SECUF, https://cstr.cn/31123.02.SECUF). We thank ISIS Facility for beam time (Grant No. RB2310088).[48]

References

[1] Balents L 2010 *Nature* **464** 199
[2] Savary L and Balents L 2017 *Rep. Prog. Phys.* **80** 016502
[3] Zhou Y, Kanoda K and Ng T K 2017 *Rev. Mod. Phys.* **89** 025003
[4] Broholm C, Cava R J, Kivelson S A, Nocera D G, Norman M R and Senthil T 2020 *Science* **367** 263
[5] Norman M R 2016 *Rev. Mod. Phys.* **88** 041002
[6] Chen G, Kee H Y and Kim Y B 2016 *Phys. Rev. B* **93** 245134
[7] Chen G and Lee P A 2018 *Phys. Rev. B* **97** 035124
[8] Schaffer R, Huh Y, Hwang K and Kim Y B 2017 *Phys. Rev. B* **95** 054410
[9] Repellin C, He Y C and Pollmann F 2017 *Phys. Rev. B* **96** 205124
[10] Iqbal Y, Poilblanc D, Thomale R and Becca F 2018 *Phys. Rev. B* **97** 115127

[11] Yao X P, Zhang X T, Kim Y B, Wang X and Chen G 2020 *Phys. Rev. Research* **2** 043424

[12] Nikolaev S A, Solovyev I V and Streltsov S V 2021 *npj Quantum Mater.* **6** 25

[13] Weber L, Caci N and Wessel S 2022 *Phys. Rev. B* **106** 035141

[14] Aidoudi F H, Aldous D W, Goff R J, Slawin A M Z, Attfield J P, Morris R E and Lightfoot P 2011 *Nat. Chem.* **3** 801

[15] Orain J C, Bernu B, Mendels P, Clark L, Aidoudi F H, Lightfoot P, Morris R E and Bert F 2017 *Phys. Rev. Lett.* **118** 237203

[16] Sheckelton J P, Foronda F R, Pan L, Moir C, McDonald R D, Lancaster T, Baker P J, Armitage N P, Imai T, Blundell S J and McQueen T M 2014 *Phys. Rev. B* **89** 064407

[17] Mourigal M, Fuhrman W T, Sheckelton J P, Wartelle A, Rodriguez-Rivera J A, Abernathy D L, McQueen T M and Broholm C L 2014 *Phys. Rev. Lett.* **112** 027202

[18] Haraguchi Y, Michioka C, Imai M, Ueda H and Yoshimura K 2015 *Phys. Rev. B* **92** 014409

[19] Akbari-Sharbaf A, Sinclair R, Verrier A, Ziat D, Zhou H D, Sun X F and Quilliam J A 2018 *Phys. Rev. Lett.* **120** 227201

[20] Iida K, Yoshida H, Okabe H, Katayama N, Ishii Y, Koda A, Inamura Y, Murai N, Ishikado M, Kadono R and Kajimoto R 2019 *Sci. Rep.* **9** 1826

[21] Chen Q, Sinclair R, Akbari-Sharbaf A, Huang Q, Dun Z, Choi E S, Mourigal M, Verrier A, Rouane R, Bazier-Matte X, Quilliam J A, Aczel A A and Zhou H D 2022 *Phys. Rev. Materials* **6** 044414

[22] Wyckoff K E, Kautzsch L, Kaufman J L, Ortiz B R, Kallistova A, Pokharel G, Liu J, Taddei K M, Wiaderek K M, Lapidus S H, Wilson S D, der Ven A V and Seshadri R 2023 *Chem. Mater.* **35** 4945

[23] Haraguchi Y, Michioka C, Ishikawa M, Nakano Y, Yamochi H, Ueda H and Yoshimura K 2017 *Inorg. Chem.* **56** 3483

[24] Sheckelton J P, Plumb K W, Trump B A, Broholm C L and McQueen T M 2017 *Inorg. Chem. Front.* **4** 481

[25] Gao S, Zhang S, Wang C, Yan S, Han X, Ji X, Tao W, Liu J, Wang T, Yuan S, Qu G, Chen Z, Zhang Y, Huang J, Pan M, Peng S, Hu Y, Li H, Huang Y, Zhou H, Meng S, Yang L, Wang Z, Yao Y, Chen Z, Shi M, Ding H, Yang H, Jiang K, Li Y, Lei H, Shi Y, Weng H and Qian T 2023 *Phys. Rev. X* **13** 041049

[26] Zhang Y, Gu Y, Weng H, Jiang K and Hu J 2023 *Phys. Rev. B* **107** 035126

[27] Grytsiuk S, Katsnelson M I, van Loon E G and Rösner M 2024 *npj Quantum Mater.* **9** 8

[28] Regmi S, Sakhya A P, Fernando T, Zhao Y, Jeff D, Sprague M, Gonzalez F, Bin Elius I, Mondal M I, Valadez N, Jarrett D, Agosto A, Yang J, Chu J H, Khondaker S I, Xu X, Cao T and Neupane M 2023 *Phys. Rev. B* **108** L121404

[29] Liu B, Zhang Y, Han X, Sun J, Zhou H, Li C, Cheng J, Yan S, Lei H, Shi Y, Yang H and Li S 2024 *J. Phys.: Condens. Matter* **36** 155602

[30] Feng Z, Li Z, Meng X, Yi W, Wei Y, Zhang J, Wang Y C, Jiang W, Liu Z, Li S, Liu F, Luo J, Li S, Zheng G, Meng Z Y, Mei J W and Shi Y 2017 *Chin. Phys. Lett.* **34** 077502

[31] Hayano R, Uemura Y, Imazato J, Nishida N, Yamazaki T and Kubo R 1979 *Phys. Rev. B* **20** 850

[32] Mendels P, Bert F, de Vries M A, Olariu A, Harrison A, Duc F, Trombe J, Lord F J, Amato A and Baines C 2007 *Phys. Rev. Lett.* **98** 077204

[33] Bert F 2014 *Collection SFN* **13** 03001

[34] Keren A, Bazalitsky G, Campbell I and Lord J S 2001 *Phys. Rev. B* **64** 054403

[35] Keren A, Gardner J S, Ehlers G, Fukaya A, Segal E and Uemura Y J 2004 *Phys. Rev. Lett.* **92** 107204

[36] Kermarrec E, Mendels P, Bert F, Colman R H, Wills A S, Strobel P, Bonville P, Hillier A and Amato A 2011 *Phys. Rev. B* **84** 100401

[37] Lee S, Lee C H, Berlie A, Hillier A D, Adroja D T, Zhong R, Cava R J, Jang Z H and Choi K Y 2021 *Phys. Rev. B* **103** 024413

[38] Lee J, Jin K H and Yeom H W 2021 *Phys. Rev. Lett.* **126** 196405

[39] Ding L, Manuel P, Bachus S, Grußler F, Gegenwart P, Singleton J, Johnson R D, Walker H C, Adroja D T, Hillier A D and Tsirlin A A 2019 *Phys. Rev. B* **100** 144432

[40] Li Y, Adroja D, Biswas P K, Baker P J, Zhang Q, Liu J, Tsirlin A A, Gegenwart P and Zhang Q 2016 *Phys. Rev. Lett.* **117** 097201

[41] Clark L, Orain J C, Bert F, De Vries M A, Aidoudi F H, Morris R E, Lightfoot P, Lord J S, Telling M T F, Bonville P, Attfield J P, Mendels P and Harrison A 2013 *Phys. Rev. Lett.* **110** 207208

[42] Khuntia P, Bert F, Mendels P, Koteswararao B, Mahajan A V, Baenitz M, Chou F C, Baines C, Amato A and Furukawa Y 2016 *Phys. Rev. Lett.* **116** 107203

[43] Balz C, Lake B, Reuther J, Luetkens H, Schönemann R, Herrmannsdörfer T, Singh Y, Islam A T M N, Wheeler E M, Rodriguez-Rivera J A, Guidi T, Simeoni G G, Baines C and Ryll H 2016 *Nat. Phys.* **12** 942

[44] Lee W J, Do S H, Yoon S, Lee S, Choi Y S, Jang D J, Brando M, Lee M, Choi E S, Ji S, Jang Z H, Suh B J and Choi K Y 2017 *Phys. Rev. B* **96** 014432

[45] Sarkar R, Schlender P, Grinenko V, Haeussler E, Baker P J, Doert T and Klauss H H 2019 *Phys. Rev. B* **100** 241116

[46] Kundu S, Shahee A, Chakraborty A, Ranjith K M, Koo B, Sichelschmidt J, Telling M T F, Biswas P K, Baenitz M, Dasgupta I, Pujari S and Mahajan A V 2020 *Phys. Rev. Lett.* **125** 267202

[47] Bhattacharya K, Mohanty S, Hillier A D, Telling M T F, Nath R and Majumder M 2024 *Phys. Rev. B* **110** L060403

[48] Li *et al.* 2024 *Investigating possible quantum-spin-liquid state in Nb3Cl8 using Muon spin relaxation* (STFC ISIS Neutron and Muon Source)